

Topological dark energy from black-hole formations and mergers through the gravity-thermodynamics approach

Stylianos A. Tsilioukas,^{1,2,*} Nicholas Petropoulos,^{1,†} and Emmanuel N. Saridakis^{2,3,4,‡}

¹*Department of Physics, University of Thessaly, 35100 Lamia, Greece*

²*National Observatory of Athens, Lofos Nymfon, 11852 Athens, Greece*

³*CAS Key Laboratory for Researches in Galaxies and Cosmology, Department of Astronomy, University of Science and Technology of China, Hefei, Anhui 230026, P.R. China*

⁴*Departamento de Matemáticas, Universidad Católica del Norte, Avda. Angamos 0610, Casilla 1280 Antofagasta, Chile*

We apply the gravity-thermodynamics approach in the case of Einstein-Gauss-Bonnet theory, and its corresponding Wald-Gauss-Bonnet entropy, which due to the Chern-Gauss-Bonnet theorem it is related to the Euler characteristic of the Universe topology. However, we consider the realistic scenario where we have the formation and merger of black holes that lead to topology changes, which induce entropy changes in the Universe horizon. We extract the modified Friedmann equations and we obtain an effective dark energy sector of topological origin. We estimate the black-hole formation and merger rates starting from the observed star formation rate per redshift, which is parametrized very efficiently by the Madau-Dickinson form, and finally we result to a dark-energy energy density that depends on the cosmic star formation rate density, on the fraction f_{BH} of stars forming black holes, on the fraction of black holes f_{merge} that eventually merge, on the fraction f_{bin} of massive stars that are in binaries, on the average mass of progenitor stars that will evolve to form black holes $\langle m_{\text{prog}} \rangle$, as well as on the Gauss-Bonnet coupling constant. We investigate in detail the cosmological evolution, obtaining the usual thermal history. Concerning the dark-energy equation-of-state parameter, we show that at intermediate redshifts it exhibits phantom-like or quintessence-like behavior according to the sign of the Gauss-Bonnet coupling, while at early and late times it tends to the cosmological constant value. Finally, we study the effect of the other model parameters, showing that for the whole allowed observationally estimated ranges, the topological dark-energy equation-of-state parameter remains within its observational bounds.

I. INTRODUCTION

According to extensive observational evidence from various origins, the Universe has recently entered a phase of accelerated expansion [1–6]. In order to explain this behavior two main directions have been pursued. The first is to retain general relativity as the gravitational framework while introducing new energy components, such as the dark energy sector [7, 8]. The second involves constructing modified and extended theories of gravity by altering the left-hand side of Einstein field equations, adding correction terms to the standard Einstein-Hilbert action [9–12]. Such modified gravity theories not only address cosmological issues but also offer improved quantum behavior [13], given that general relativity is non-renormalizable [14]. Specifically, incorporating higher-order curvature terms into the Einstein-Hilbert Lagrangian tends to eliminate divergences [15], and among all higher-order terms the Gauss-Bonnet (GB) combination is special since it is topologically invariant in 4 dimensions and thus plays a significant role in heterotic string theory [15–18] and in M-theory [19].

Beyond the aforementioned approaches to modified gravity theories, there exists a well-known conjecture that gravity can be described through the laws of thermo-

dynamics [20–22]. This concept is inspired from black-hole thermodynamics, where a black hole (BH) is assigned a specific temperature and entropy, dependent on its horizon [23]. The “thermodynamics of spacetime” conjecture [20] draws an analogy from BH horizon thermodynamics to the Universe horizon at cosmological scales. In particular, if one applies the first law of thermodynamics in the apparent horizon one can obtain the Friedmann equations [24–26], and vice versa the Friedmann equations can be expressed as the first law of thermodynamics. This procedure has been applied successfully both in the case of general relativity and as well as in modified theories of gravity [27–38], where in the latter case one should use the corresponding modified entropy relation.

In the present work we are interested in applying the gravity-thermodynamics approach in the case where the gravitational action is extended by the GB term and the corresponding entropy is extended by the Wald-Gauss-Bonnet entropy [39, 40], a term dependent on the BH horizon topology. However, we are interested in considering the realistic scenario where in the Universe we have the formation and merger of black holes, that lead to topology changes which induce entropy changes in the Universe horizon. Hence, applying the gravity-thermodynamics analysis one could extract modified Friedmann equations, with an effective, dark energy sector of topological origin, depending on the black-hole formation and merger rates.

The plan of this manuscript is the following: In sec-

* tsilioukas@sch.gr

† npetropoulos@uth.gr

‡ msaridak@noa.gr

tion II we review the standard gravity-thermodynamics approach, and then we apply it in the case of Einstein-Gauss-Bonnet theory, extracting the modified Friedmann equations. In section III we first provide an estimation for the BH formation and merging rates using the star formation rate as the starting point, and then we proceed to the detailed cosmological applications of specific scenarios, focusing on the behavior of the dark-energy and matter density parameters, of the effective dark-energy equation-of-state parameter, and of the deceleration parameter. Finally in IV we summarize our results and we conclude.

II. MODIFIED COSMOLOGY FROM WALD-GAUSS-BONNET ENTROPY

In this section we present the scenario at hand, extracting the modified Friedmann equations by applying the first law of thermodynamics to the Universe using the Wald-Gauss-Bonnet entropy. We start by considering a homogeneous and isotropic Friedmann-Robertson-Walker (FRW) geometry with metric

$$ds^2 = -dt^2 + a^2(t) \left(\frac{dr^2}{1 - kr^2} + r^2 d\Omega^2 \right), \quad (1)$$

where $a(t)$ is the scale factor, and $k = 0, +1, -1$ corresponds to flat, closed, and open spatial geometry, respectively.

A. Friedmann equations as the first law of thermodynamics

To extract the Friedmann equations in general relativity from the first law of thermodynamics, we consider an expanding Universe filled with a matter perfect fluid, with energy density ρ_m and pressure p_m . As a boundary, one uses the apparent horizon [24–26]

$$\tilde{r}_A = \frac{1}{\sqrt{H^2 + \frac{k}{a^2}}}, \quad (2)$$

where $H = \frac{\dot{a}}{a}$ is the Hubble parameter. The apparent horizon is a marginally trapped surface with vanishing expansion, and it is a causal horizon associated with gravitational entropy and surface gravity [20–22]. The temperature attributed to the apparent horizon is

$$T_h = \frac{1}{2\pi\tilde{r}_A}, \quad (3)$$

and the entropy in general relativity is given by the standard Bekenstein-Hawking relation

$$S_h = \frac{A}{4G}, \quad (4)$$

where $A = 4\pi\tilde{r}_A^2$ is the area of the apparent horizon. Assuming that the Universe fluid acquires the same temperature with the horizon after equilibrium, the heat flow crossing the horizon during an infinitesimal time interval dt can be found to be [24]

$$\delta Q = -dE = A(\rho_m + p_m)H\tilde{r}_A dt. \quad (5)$$

Since the first law of thermodynamics states that $-dE = TdS$, using the temperature and entropy from (3) and (4) we find

$$-4\pi G(\rho_m + p_m) = \dot{H} - \frac{k}{a^2}. \quad (6)$$

Finally, considering that the matter fluid satisfies the conservation equation

$$\dot{\rho}_m + 3H(\rho_m + p_m) = 0, \quad (7)$$

integrating (6) we obtain

$$\frac{8\pi G\rho_m}{3} = H^2 + \frac{k}{a^2} - \frac{\Lambda}{3}, \quad (8)$$

with Λ the integration constant. Equations (8) and (6) are nothing else but the two Friedmann equations, with the integration constant Λ playing the role of the cosmological constant.

B. Wald-Gauss-Bonnet entropy

In the previous subsection we saw how one can extract the Friedmann equations through the gravity-thermodynamics conjecture. As we mentioned in the Introduction, the same procedure can be applied to modified gravity theories by changing the entropy relation to the one of the specific modified gravity at hand.

One of the widely studied higher-order theories is the Gauss-Bonnet one, due its topological significance [41, 42]. The total action in four dimensions consists of the Einstein-Hilbert and the Gauss-Bonnet (GB) term, namely

$$I = \frac{1}{16\pi G} \int d^4x \sqrt{-g} (R + \tilde{\alpha}\mathcal{G}), \quad (9)$$

where R is the Ricci scalar, \mathcal{G} is the GB term, defined as

$$\mathcal{G} = R^2 - 4R_{\mu\nu}R^{\mu\nu} + R_{\mu\nu\rho\sigma}R^{\mu\nu\rho\sigma}, \quad (10)$$

and $\tilde{\alpha}$ is the GB coupling constant.

The presence of the GB term modifies the expression for the BH entropy. In particular, the Wald-Noether charge method [39, 40] can be used to derive a horizon entropy S satisfying the first law of thermodynamics for any first-order spacetime perturbation. For any diffeomorphism invariant theory of gravity described by a Lagrangian L , the Wald entropy of a stationary BH with a regular bifurcation surface is given by [40, 43]

$$S_{\text{Wald}} = -\frac{1}{8} \int_B \frac{\partial L}{\partial R_{ijkl}} \epsilon_{ij} \epsilon_{kl} \sqrt{\sigma} d^{D-2}x, \quad (11)$$

where the integration is over any $(D - 2)$ -dimensional spacelike cross-section B of the horizon, and ϵ_{ij} is the binormal on such a cross-section, normalized as $\epsilon_{ij}\epsilon^{ij} = -2$. For the Einstein-Gauss-Bonnet action (9), the Wald entropy becomes

$$S_{\text{WGB}} = \frac{1}{4} \int_B \left(1 + 2\tilde{\alpha}^{(D-2)} R\right) \sqrt{\sigma} d^{D-2}x, \quad (12)$$

where ${}^{(D-2)}R$ is the Ricci curvature associated with the $(D - 2)$ -dimensional cross-section of the horizon. Applying to $D = 4$ dimensions the expression of the Wald-Gauss-Bonnet (WGB) entropy becomes

$$S_{\text{WGB}} = \frac{A}{4G} + \frac{\tilde{\alpha}}{2G} \int_h d^2x \sqrt{\sigma} \mathcal{R}, \quad (13)$$

where \mathcal{R} is the Ricci scalar of the induced metric on the horizon h .

Now, according to the Chern-Gauss-Bonnet theorem [44], the integral of the Ricci scalar \mathcal{R} over the two-dimensional horizon h equals 4π times the Euler characteristic $\chi(h)$ of the horizon, namely

$$\int_h d^2x \sqrt{\sigma} \mathcal{R} = 4\pi \chi(h). \quad (14)$$

The Euler characteristic χ is defined as the alternating sum of the Betti numbers B_p of a manifold M , namely $\chi(M) = \sum_p (-1)^p B_p$ [45], where the Betti numbers are defined as the dimension of the p^{th} de Rahm cohomology group $H^p(M)$, i.e. $B_p = \dim H^p(M)$ [46, 47]. Hence, combining (13) and (14) we find that the entropy for a BH in the presence of the Einstein-Gauss-Bonnet terms is [48]

$$S_{\text{WGB}} = \frac{A}{4G} + \frac{2\pi\tilde{\alpha}}{G} \chi(h). \quad (15)$$

Thus, the Wald-Gauss-Bonnet entropy can be interpreted as a sum of an area term (the Bekenstein-Hawking one) and a topological term (the Euler characteristic of the horizon), namely

$$S_{\text{SGB}} = S_{\text{area}} + S_{\text{top}}. \quad (16)$$

Nevertheless, the above consideration may lead to a potential problem when we have black hole mergers. As it was discussed in [48], while in the case of general relativity the corresponding Bekenstein-Hawking entropy increases, the Wald entropy of the Einstein-Gauss-Bonnet theory exhibits a decrease of topological origin. In particular, as we saw above, in the case of the GB term the corresponding entropy (15) depends on the Euler characteristic of the horizon $\chi(h)$. Since the horizon of a BH is a two-dimensional sphere S^2 , during the merger of two BHs their horizons merge too, as illustrated in Fig. 1. Before the merger, the spacetime contains two horizons, i.e.

$$\chi_{\text{in}} = \chi(S^2) + \chi(S^2) = 4, \quad (17)$$

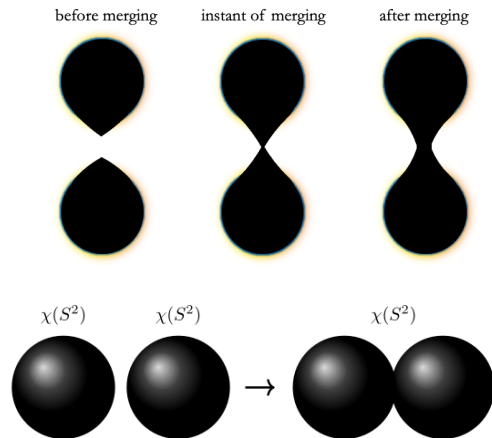


FIG. 1. The topology and the Euler characteristic change of a black hole merger.

while after the merger there is only one horizon, namely

$$\chi_f = \chi(S^2) = 2, \quad (18)$$

and therefore during a black hole merger one obtains an Euler characteristic change

$$\delta\chi_h = \chi_f - \chi_{\text{in}} = -2. \quad (19)$$

Hence, if one considers Einstein-Gauss-Bonnet theory and the extended entropy (15) it is straightforward to see that for $\tilde{\alpha} > 0$, the topological transition during the BH merger induces a decrease in the topological part of Wald entropy $\Delta S_{\text{top}} \leq 0$, resulting to a violation of the second law (in the same lines, when a BH horizon forms from gravitational collapse an increase of the Wald entropy is induced by the topological transition $\delta\chi = 2$). On the other hand, in the case $\tilde{\alpha} < 0$ there is an increase of Wald entropy during BH mergers and a decrease during a BH formation.

Since the above violation originates from the decrease of the BHs horizon Euler characteristic, and since the decrease is an instantaneous integer jump which cannot be compensated by a continuous procedure [48], one possible way to resolve the second law violation is to assume that a similar process exists that compensates the decrease of the topological part of the entropy. Having in mind the discussion of the gravity-thermodynamics conjecture and that the BH horizon and the apparent horizon are causal horizons, we assume here that the topology of the causally connected boundaries remains constant. In particular, the apparent horizon is the external boundary while the BH horizons are the internal ones, and therefore we can define the total boundary as $\partial M = \mathcal{H} \cup_{i=1}^N h_i$ and then apply the calculation for the Euler characteristics as

$$\chi(\partial M) = \chi(\mathcal{H}) + \sum_{i=1}^N \chi(h_i). \quad (20)$$

Since the overall boundary topology remains constant $\delta\chi(\partial M) = 0$ then $\delta\chi(\mathcal{H}) = -\delta\sum_{i=1}^N\chi(h_i)$.

Now, the change in the Euler characteristic of BH horizons at every BH formation from collapse is $\delta\chi(h) = 2$, while at every merger it is $\delta\chi(h) = -2$. Therefore, if δN_{form} BH formations and δN_{merg} BH mergers occur, then the corresponding change of the Euler characteristic of the apparent horizon will be

$$\delta\chi(\mathcal{H}) = -2(\delta N_{form} - \delta N_{merg}). \quad (21)$$

By demanding that the total topology of the causally connected boundaries remains constant, each time a BH horizon is formed the Euler characteristic of the apparent horizon decreases by 2, while each time two BH horizons merge into one the Euler characteristic of the apparent horizon increases by 2. For two-dimensional surfaces the Euler characteristic is given by [49]

$$\chi = 2 - 2g - b, \quad (22)$$

where g is the genus, the number of handles the surface possesses (torus-like holes) and b is the number of boundary components puncture-like holes. An interpretation of (21) according to (22) could be that each time a BH horizon is formed two compensating puncture disks appear (open up) on the causal horizon, while each time two BH horizons merge two disk punctures disappear (close up) on the causal horizon, as it has been illustrated in Fig. 2. We mention here that the connection between the Universe horizon (the largest scale of the theory) and small scales is known to hold according to the holographic principle [50–54], with a famous cosmological application being the holographic dark energy [55–66]. In similar lines, in the following we will obtain a dark energy sector of topological nature.

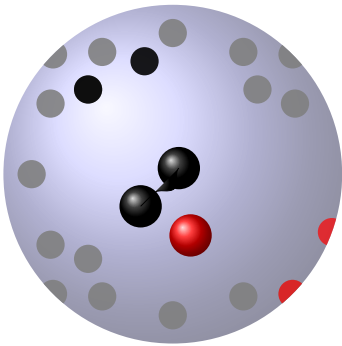


FIG. 2. *Each time a BH horizon is formed from gravitational collapse (the red sphere), two corresponding puncture holes appear on the horizon (red disks). Similarly, each time two BH horizons merge (black binary), two corresponding puncture holes close up on the apparent horizon (black disks). The grey holes indicate an arbitrary number of disk punctures excess on the horizon, since only a fraction of the BHs merge.*

In summary, a first consequence of the above considerations is that the second law of thermodynamics is satisfied

by Hawking area theorem [67]. A second consequence is that the topology of the causal horizon becomes dynamical, thus a new term of topological origin appears when one derives the Friedmann equations in the spacetime-thermodynamics framework for the Wald-Gauss-Bonnet entropy, as we will see in the next subsection.

C. Modified Friedmann equations form Wald-Gauss-Bonnet entropy

In subsection II A we showed how the standard Friedmann equations can be obtained from the first law of thermodynamics in the case of Bekenstein-Hawking entropy that corresponds to general relativity. In the present subsection we will follow the same procedure for the case of the Wald-Gauss-Bonnet entropy discussed in subsection II B.

Differentiating the expression of the Wald-Gauss-Bonnet entropy (15), and using (2), we find

$$\frac{dS}{dt} = -\frac{2\pi\tilde{r}_A^4}{4G}H\left(\dot{H} - \frac{k}{a^2}\right) + \frac{\pi\tilde{a}}{G}\dot{\chi}(\mathcal{H}). \quad (23)$$

Thus, substituting into the first law of thermodynamics $-dE = TdS$ where dE is given by (5) and T by (3), we obtain

$$-4\pi G(\rho_m + p_m) = \left(\dot{H} - \frac{k}{a^2}\right) - 4\tilde{a}\frac{1}{H}\left(H^2 + \frac{k}{a^2}\right)^2\dot{\chi}(\mathcal{H}). \quad (24)$$

Hence, inserting the conservation equation (7) and integrating, we finally acquire

$$H^2 = \frac{8\pi G}{3}\rho_m + \frac{k}{a^2} + \frac{\Lambda}{3} + 4\tilde{a}\int_0^t\left(H^2 + \frac{k}{a^2}\right)^2\dot{\chi}(H)dt. \quad (25)$$

Having in mind the discussion of the previous subsection, if we define the active BH number as the difference between BH formations and BH mergers, namely

$$N = N_{form} - N_{merg}, \quad (26)$$

we can express $\dot{\chi}(\mathcal{H})$ according to (21). Thus, inserting into (25) we finally obtain

$$H^2 = \frac{8\pi G}{3}\rho_m + \frac{k}{a^2} + \frac{\Lambda}{3} - 8\tilde{a}\int_0^t\left(H^2 + \frac{k}{a^2}\right)^2\frac{dN}{dt}dt. \quad (27)$$

Interestingly enough, through the application of the gravity-thermodynamics conjecture in the case of Wald-Gauss-Bonnet entropy, we have obtained modified Friedmann equations depending on the BH formations and mergers and on the GB coupling constant. Note that in the case where the Gauss-Bonnet term is absent one recovers the standard cosmological paradigm, which was expected since in this case the Wald-Gauss-Bonnet entropy (15) recovers the standard Bekenstein-Hawking one, and thus the Euler characteristic change does not

have any effect on the entropy and hence on the gravity-thermodynamics conjecture. Finally, note that while Einstein-Gauss-Bonnet theory in 4 dimensions leads to the same field equations with general relativity, its implementation within the gravity-thermodynamics approach does lead to extra terms due to the entropy changes caused by the topology changes brought about by the evolution of the Einstein-Gauss-Bonnet black holes.

We can rewrite equations (27) and (24) as

$$H^2 = \frac{8\pi G}{3}(\rho_m + \rho_{DE}) \quad (28)$$

$$H^2 + \dot{H} = -\frac{4\pi G}{3}(\rho_m + 3p_m + \rho_{DE} + 3p_{DE}) \quad (29)$$

by introducing an effective dark energy sector of topological origin, with energy density and pressure defined as

$$\rho_{DE} = \frac{3}{8\pi G} \left(\frac{\Lambda}{3} - 8\tilde{a} \int_0^t \left(H^2 + \frac{k}{a^2} \right)^2 \frac{dN}{dt} dt \right), \quad (30)$$

and

$$p_{DE} = -\frac{1}{4\pi G} \left[\frac{\Lambda}{2} + 8\tilde{a} \frac{1}{H} \left(H^2 + \frac{k}{a^2} \right)^2 \frac{dN}{dt} - 12\tilde{a} \int_0^t \left(H^2 + \frac{k}{a^2} \right)^2 \frac{dN}{dt} dt \right]. \quad (31)$$

Additionally, we define the effective dark-energy equation-of-state parameter as $w_{DE} \equiv \frac{p_{DE}}{\rho_{DE}}$, leading to

$$w_{DE} = -1 + \frac{2\tilde{a} \left(H^2 + \frac{k}{a^2} \right)^2 \frac{dN}{dt}}{H \left(\frac{\Lambda}{4} - 6\tilde{a} \int_0^t \left(H^2 + \frac{k}{a^2} \right)^2 \frac{dN}{dt} dt \right)}. \quad (32)$$

Lastly, from (28), (29), and assuming that the matter sector is conserved, i.e. $\dot{\rho}_m + 3H(\rho_m + p_m) = 0$, we acquire that the effective dark energy sector is conserved too, namely $\dot{\rho}_{DE} + 3H(\rho_{DE} + p_{DE}) = 0$.

III. COSMIC EVOLUTION

In the previous section we applied the gravity-thermodynamics conjecture in the case of Wald-Gauss-Bonnet entropy, and we obtained modified Friedmann equations and an effective dark energy sector of topological origin, dependent on the black hole formation and merger. Therefore, we can now proceed to the investigation of the cosmological implications.

For convenience we use the redshift z as the independent variable, defined as $1 + z = a_0/a$, and we set the current scale factor to $a_0 = 1$. Additionally, we will focus on dust matter (namely with $p_m = 0$), which implies $\rho_m = \rho_{m0}(1+z)^3$, with ρ_{m0} the matter energy density at

present. As usual, we introduce the dimensionless density parameters

$$\Omega_{DE} = \frac{8\pi G}{3H^2} \rho_{DE}, \quad (33)$$

and

$$\Omega_m = \frac{8\pi G}{3H^2} \rho_m. \quad (34)$$

Inserting the above into (30) we obtain

$$\rho_{DE}(z) = \frac{3}{8\pi G} \left\{ \frac{\Lambda}{3} - 8\tilde{a} \int_{z_0}^z [H^2 + k(1+z)^2]^2 \frac{dN}{dz} dz \right\}, \quad (35)$$

while (32) gives

$$w_{DE}(z) = -1 - \frac{2\tilde{a} [H^2 + k(1+z)^2]^2 (1+z) \frac{dN}{dz}}{\frac{\Lambda}{4} - 6\tilde{a} \int_{z_0}^z [H^2 + k(1+z)^2]^2 \frac{dN}{dz} dz}. \quad (36)$$

Lastly, we can introduce the deceleration parameter $q \equiv -1 - \dot{H}/H^2$, which in terms of redshift becomes

$$q(z) = -1 + \frac{(1+z)}{H(z)} \frac{dH(z)}{dz}. \quad (37)$$

As we see, the effective dark energy density depends on the black hole formation and merger rates, namely on $\frac{dN}{dz}$. Thus, in the following subsection we provide an estimation for its value.

A. Black hole formation and merger rates

Let us estimate the rate of the number of BHs that form and merge per redshift. In order to achieve that we need to estimate independently the black-hole formation rate and the black-hole merger rate.

1. Estimating the black-hole formation rate from the star formation rate

Since black holes typically evolve from massive stars, it is commonly assumed that the formation rate of BHs (BHFR) is proportional to the cosmic star formation rate (SFR) [68–70]. The cosmic star formation rate density is presented in Fig. 3, and its best fit form is given by Madau and Dickinson [71] as

$$\psi(z) = 0.015 \frac{(1+z)^{2.7}}{1 + [(1+z)/2.9]^{5.6}} M_{\odot} \text{year}^{-1} \text{Mpc}^{-3}. \quad (38)$$

To estimate the BHFR from the SFR, we will consider the fraction of stellar mass that ends up as BH progenitors. This fraction depends on the initial mass function (IMF) and the mass range of stars that collapse

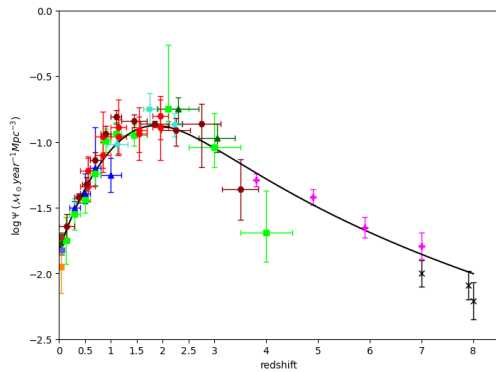


FIG. 3. The history of cosmic star formation rate from [71]. On top of the data points, the black solid curve represents the best fit to the data, namely the Madau-Dickinson form (38).

into BHs. Assuming a Salpeter IMF [72], which gives $\xi(m) \propto m^{-2.35}$, and considering stars with initial masses $m > 25 M_{\odot}$ as BH progenitors, the fraction f_{BH} of stellar mass forming BH progenitors is

$$f_{\text{BH}} = \frac{\int_{25 M_{\odot}}^{\infty} m \xi(m) dm}{\int_{0.1 M_{\odot}}^{\infty} m \xi(m) dm}, \quad (39)$$

and it represents the fraction of total stellar mass that goes into stars massive enough to eventually form BHs. According to various studies, f_{BH} ranges from approximately 0.001 to 0.05 [73, 74].

The average mass of progenitor stars that will evolve to form BHs, namely $\langle m_{\text{prog}} \rangle$, is typically in the range of $25 M_{\odot}$ to $40 M_{\odot}$ [75, 76]. Thus, the number rate density of BHs formed per unit volume per unit time, $\dot{\rho}_{\text{BH}}(z)$, is given by

$$\dot{\rho}_{\text{BH}}(z) = f_{\text{BH}} \frac{\psi(z)}{\langle m_{\text{prog}} \rangle}. \quad (40)$$

Hence, the number rate of BHs that form inside the apparent horizon of volume $\tilde{V}_A = \frac{4\pi}{3} \tilde{r}_A^3$, will be $\dot{N}_{\text{BH}} = \dot{\rho}_{\text{BH}} \tilde{V}_A$, and thus for a flat Universe from (2) we have $\tilde{r}_A = 1/H$, which leads to

$$\dot{N}_{\text{BH}}(z) = \frac{4\pi}{3} f_{\text{BH}} \frac{\psi(z)}{\langle m_{\text{prog}} \rangle H^3(z)}. \quad (41)$$

Finally, expressing the number rate of BHs formation per redshift instead of time, using $|dt/dz| = 1/H(z)(1+z)$, yields

$$\frac{dN_{\text{BH}}(z)}{dz} = \frac{4\pi}{3} f_{\text{BH}} \frac{\psi(z)}{\langle m_{\text{prog}} \rangle (1+z) H^4(z)}. \quad (42)$$

2. Estimating the black-hole merger rate from the black-hole formation rate

The binary black hole merger rate (BHMR) can also be assumed to be proportional to SFR. Nevertheless, ambi-

guities arise in this simplified approach as the formation efficiency of compact object is metallicity-dependent and BH formation and binary black hole merging may occur with a significant delay relative to the star formation epoch [77]. We are going to estimate approximately the BHMR from the BHFR by considering as main factors the fraction of massive stars that are in binary systems and the merger efficiency. Observations suggest that a significant fraction of massive stars are in binaries, which is estimated around $f_{\text{bin}} \approx 0.7$ [78]. Nevertheless, not all binary black holes will merge within the age of the Universe. The merger efficiency f_{merge} accounts for the fraction of binary black holes that will eventually merge within a Hubble time. This efficiency depends on factors such as the initial separation and eccentricity of the binary system, and it is estimated to be between 0.01 and 0.1 [79–81]. Therefore, the black hole merger rate with respect to redshift will be

$$\frac{dN_{\text{BHMR}}(z)}{dz} = f_{\text{bin}} \times f_{\text{merge}} \times \frac{dN_{\text{BH}}(z)}{dz}, \quad (43)$$

which using (42) yields

$$\frac{dN_{\text{BHMR}}(z)}{dz} = \frac{4\pi}{3} f_{\text{BH}} \times f_{\text{bin}} \times f_{\text{merge}} \times \frac{\psi(z)}{\langle m_{\text{prog}} \rangle H^4(z) (1+z)}. \quad (44)$$

B. Specific examples

Having estimated the black-hole formation and merger rates in (42) and (44), we can insert in (26) and obtain the expression for the rate of the active number of BHs per redshift inside the apparent horizon as

$$\frac{dN(z)}{dz} = C \frac{\psi(z)}{H^4(z) (1+z)}, \quad (45)$$

where we have defined the constant

$$C \equiv \frac{4\pi}{3} \frac{(1 - f_{\text{bin}} \times f_{\text{merge}}) f_{\text{BH}}}{\langle m_{\text{prog}} \rangle}. \quad (46)$$

Hence, inserting (45) into (28), (35) and (36) we acquire

$$H^2 = H_0^2 \Omega_{m0} (1+z)^3 + \frac{\Lambda}{3} - 8\tilde{a}C \int_{z_0}^z \frac{\psi(z)}{(1+z)} dz, \quad (47)$$

$$\rho_{DE}(z) = \frac{3}{8\pi G} \left(\frac{\Lambda}{3} - 8\tilde{a}C \int_{z_0}^z \frac{\psi(z)}{(1+z)} dz \right), \quad (48)$$

and

$$w_{DE}(z) = -1 - \frac{2\tilde{a}C\psi(z)}{\frac{\Lambda}{4} - 6\tilde{a}C \int_{z_0}^z \frac{\psi(z)}{(1+z)} dz}, \quad (49)$$

with H_0 the current value of the Hubble function. As we see, apart from the constants, the only dynamical

function that enters the equations is the star formation rate $\psi(z)$, which is given by (38). The integral can be evaluated in terms of the hypergeometric function ${}_2F_1(a, b; c; z)$, and gives

$$\int \frac{\psi(z)}{(1+z)} dz = 0.37037 \cdot (1+z)^{2.7} {}_2F_1(0.482143, 1.0; 1.48214; -0.00257378 \cdot (1+z)^{5.6}). \quad (50)$$

Finally, concerning the involved parameters, in Table I we display the possible values according to the literature.

TABLE I. Range of the involved parameters according to the literature.

Parameter	Value	Reference
f_{BH}	0.1% to 5%	[73, 74]
$\langle m_{prog} \rangle$	25 to 40 M_\odot	[75, 76]
f_{merge}	1% to 10%	[79-81]
f_{bin}	50% to 80%	[78, 82, 83]

1. $\tilde{\alpha} > 0$ case

We start our analysis by examining the case where the GB coupling constant $\tilde{\alpha}$ is positive. We elaborate the cosmological equations numerically, imposing $\Omega_{DE}(z=0) \equiv \Omega_{DE0} \approx 0.69$ and $\Omega_m(z=0) \equiv \Omega_{m0} \approx 0.31$ as required by observations [84]. In the upper graph of Fig. 4 we present the evolution of the dimensionless density parameters $\Omega_{DE}(z)$ and $\Omega_m(z)$. We observe that we can acquire the usual thermal history of the Universe, the standard sequence of matter and dark energy epochs, while in the asymptotic future ($z \rightarrow -1$) the Universe results to be completely dominated by dark energy. In the middle graph we draw the evolution of the dark-energy equation-of-state parameter $w_{DE}(z)$, where we can see that it lies slightly in the phantom regime for intermediate redshifts, well inside the observational bounds [84], while it approaches $w_{DE} \rightarrow -1$ in the distant past and in the asymptotic future. Finally, in the last graph of Fig. 4 we depict the deceleration parameter $q(z)$, where we can see that the transition from deceleration to acceleration occurs at $z_{tr} \approx 0.6$ in agreement with observations.

We proceed by studying the effect of the positive GB coupling constant $\tilde{\alpha}$ on the dark-energy equation-of-state parameter. In Fig. 5 we can see that for small values, namely for $0 \leq \tilde{\alpha} \leq 10^3$ in H_0 units, the scenario coincides with Λ CDM paradigm. Nevertheless, as the value of $\tilde{\alpha}$ becomes larger, $w_{DE}(z)$ enters deeper into the phantom regime peaking at $z \approx 2$, while its behavior in the distant past and asymptotic future still resembles Λ CDM one.

In order to examine the effect of the BH formation factor f_{BH} on $w_{DE}(z)$, in Fig. 6 we demonstrate its evolution for various values of f_{BH} . We can see that for the smallest value according to the literature, i.e.

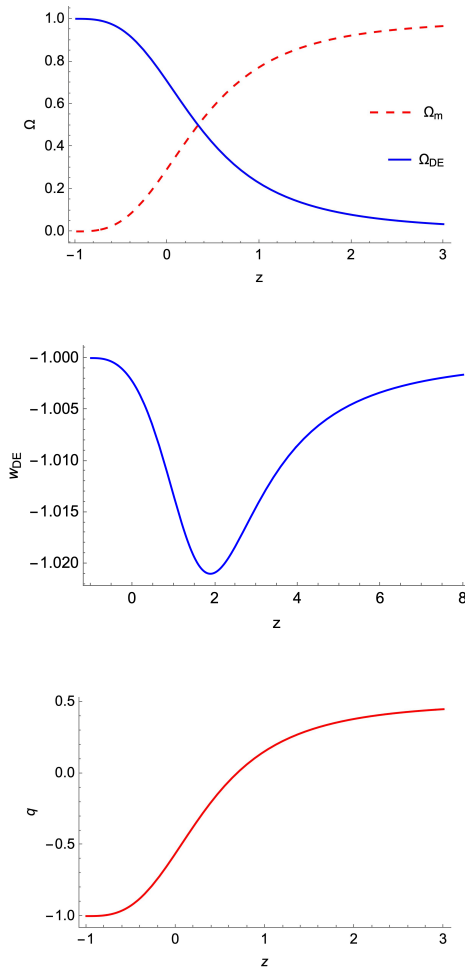


FIG. 4. Upper graph: The evolution of the dimensionless dark energy parameter Ω_{DE} (blue-solid) and the corresponding matter density parameter Ω_m (red-dashed) as a function of redshift, for the modified scenario with Wald-Gauss-Bonnet entropy, with $\tilde{\alpha} > 0$. Middle graph: The evolution of the dark energy equation of state parameter w_{DE} . Lower graph: The evolution of the deceleration parameter q . In all graphs we have used the models parameters $\tilde{\alpha} = 10^5$ (in H_0 units), $f_{BH} = 0.025$, $m_{prog} = 30M_\odot$, $f_{bin} = 0.65$, $f_{merge} = 0.05$ and we have implemented $\Omega_{DE0} = 0.69$.

$f_{BH} = 0.001$, the model tends to Λ CDM behavior. As f_{BH} increases $w_{DE}(z)$ enters deeper into the phantom regime and remains inside observational bounds [84] for the highest estimated value $f_{BH} = 0.001$. Finally, in the distant past and asymptotic future we obtain $w_{DE} \rightarrow -1$, independently of the parameter value.

Finally, we examine the behavior of $w_{DE}(z)$ with respect to the estimated range of values of the BH merging parameter f_{merge} . In Fig. 7 one can see that $w_{DE}(z)$ increases slightly as f_{merge} increases, however its effect is minor comparing to the previous parameters. Again, in the distant past and asymptotic future we have $w_{DE} \rightarrow -1$, independently of the parameter value.

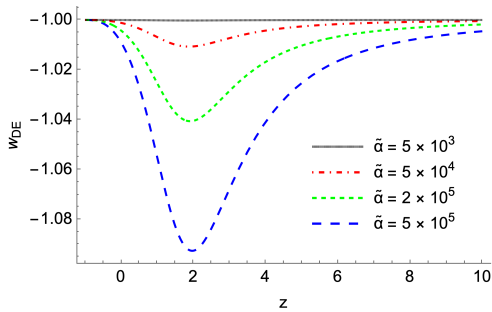


FIG. 5. The evolution of the effective dark-energy equation-of-state parameter w_{DE} for various values of positive GB coupling constant $\tilde{\alpha}$ in H_0 units. The other model parameters used in the calculation are $f_{BH} = 0.025$, $m_{prog} = 30M_{\odot}$, $f_{bin} = 0.65$, $f_{merge} = 0.05$, and we have imposed $\Omega_{DE0} = 0.69$. In all cases the density parameters exhibit similar behaviors with those presented in the upper graph of Fig. 4.

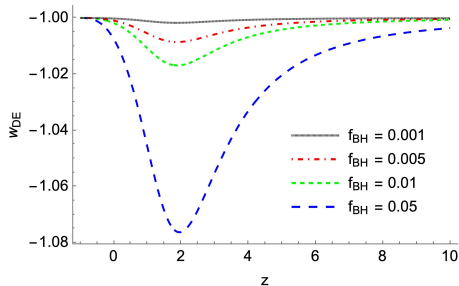


FIG. 6. The evolution of the effective dark-energy equation-of-state parameter w_{DE} for various values of the fraction of stars that form black holes f_{BH} . The other model parameters used in the calculation are $\tilde{\alpha} = 2 \times 10^5$ in H_0 units, $m_{prog} = 30M_{\odot}$, $f_{bin} = 0.65$, $f_{merge} = 0.05$ and we have imposed $\Omega_{DE0} = 0.69$. In all cases the density parameters exhibit similar behaviors with those presented in the upper graph of Fig. 4.

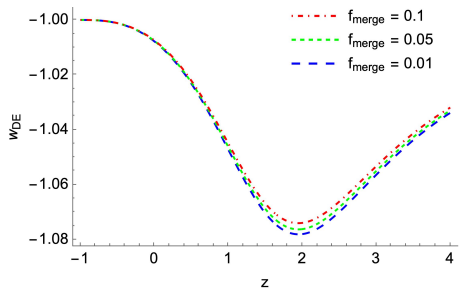


FIG. 7. The evolution of the effective dark-energy equation-of-state parameter w_{DE} for various values of the fraction of BHs that eventually merge f_{merge} . The other model parameters used in the calculation are $\tilde{\alpha} = 2 \times 10^5$ in H_0 units, $f_{BH} = 0.025$, $m_{prog} = 30M_{\odot}$, $f_{bin} = 0.65$, and we have imposed $\Omega_{DE0} = 0.69$. In all cases the density parameters exhibit similar behaviors with those presented in the upper graph of Fig. 4.

2. $\tilde{\alpha} < 0$ case

We now present the cosmological behavior for negative GB coupling constant $\tilde{\alpha} < 0$. In the upper graph

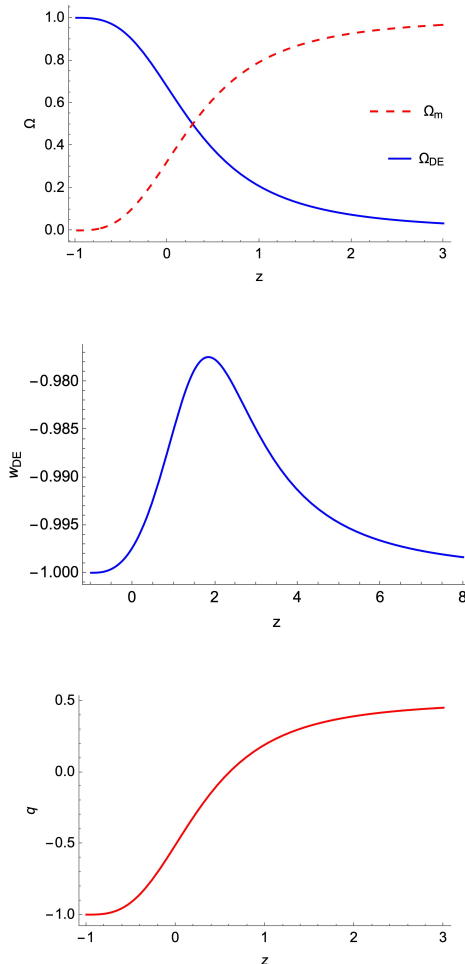


FIG. 8. Upper graph: The evolution of the dimensionless dark energy parameter Ω_{DE} (blue-solid) and the corresponding matter density parameter Ω_m (red-dashed) as a function of redshift, for the modified scenario with Wald-Gauss-Bonnet entropy, with $\tilde{\alpha} < 0$. Middle graph: The evolution of the dark energy equation of state parameter w_{DE} . Lower graph: The evolution of the deceleration parameter q . In all graphs we have used the models parameters $\tilde{\alpha} = -10^5$ (in H_0 units), $f_{BH} = 0.025$, $m_{prog} = 30M_{\odot}$, $f_{bin} = 0.65$, $f_{merge} = 0.05$ and we have implemented $\Omega_{DE0} = 0.69$.

of Fig. 8 we present the evolution of $\Omega_{DE}(z)$ and $\Omega_m(z)$, where one can see that the anticipated thermal history of the Universe and the sequence of matter and dark energy epochs are acquired. Furthermore, in the asymptotic future dark energy dominates completely, leading the Universe to a de Sitter phase. In the middle graph we observe that the dark-energy equation-of-state parameter lies in the quintessence regime ($w_{DE} > -1$) for small redshifts, peaking at $z \approx 2$, and in the asymptotic future

it approaches $w_{DE} \rightarrow -1$. Finally, in the lower graph we display the evolution of the deceleration parameter and we can see that the transition from deceleration to acceleration happens at $z_{tr} \approx 0.6$ as required.

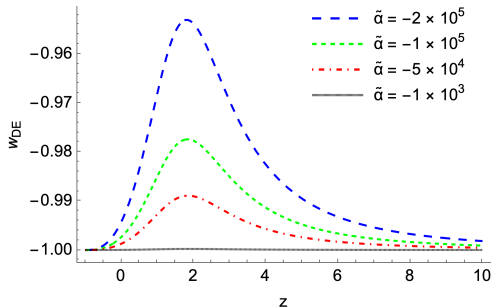


FIG. 9. The evolution of the effective dark-energy equation-of-state parameter w_{DE} for various values of negative GB coupling constant $\tilde{\alpha}$ in H_0 units. The other model parameters used in the calculation are $f_{BH} = 0.025$, $m_{prog} = 30M_{\odot}$, $f_{bin} = 0.65$, $f_{merge} = 0.05$, and we have imposed $\Omega_{DE0} = 0.69$. In all cases the density parameters exhibit similar behaviors with those presented in the upper graph of Fig. 4.

In Fig. 9 we plot w_{DE} for different values of the negative GB coupling constant. For small absolute values, namely for $-10^3 \leq \tilde{\alpha} \leq 0$ in H_0 units we retrieve Λ CDM behavior, while when the absolute value of the parameter $\tilde{\alpha}$ increases then w_{DE} enters upwards to the quintessence regime. Additionally, in Fig. 10 we draw w_{DE} for dif-

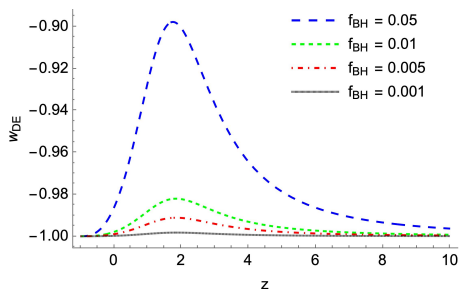


FIG. 10. The evolution of the effective dark-energy equation-of-state parameter w_{DE} for various values of the fraction of stars that form black holes f_{BH} . The other model parameters used in the calculation are $\tilde{\alpha} = -2 \times 10^5$ in H_0 units, $m_{prog} = 30M_{\odot}$, $f_{bin} = 0.65$, $f_{merge} = 0.05$, and we have imposed $\Omega_{DE0} = 0.69$. In all cases the density parameters exhibit similar behaviors with those presented in the upper graph of Fig. 4.

ferent values of the fraction f_{BH} of stars that form BHs. As we can see, for the smallest value of the estimated range, i.e. for $f_{BH} = 0.001$, w_{DE} tends to Λ CDM behavior, while as the values of f_{BH} increases, $w_{DE}(z)$ enters higher to the quintessence regime. However, for the whole allowed f_{BH} range showed in Table I, $w_{DE}(z)$ remains always inside the observational bound [84]. Lastly,

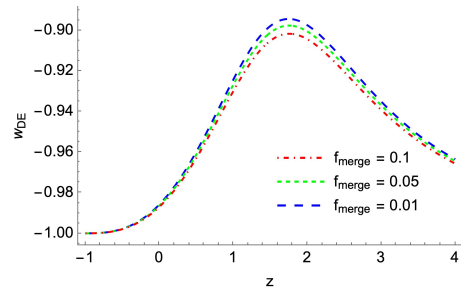


FIG. 11. The evolution of the effective dark-energy equation-of-state parameter w_{DE} for various values of the fraction of black holes that eventually merge f_{merge} . The other model parameters used in the calculation are $\tilde{\alpha} = -2 \times 10^5$ in H_0 units, $f_{BH} = 0.025$, $m_{prog} = 30M_{\odot}$, $f_{bin} = 0.65$, and we have imposed $\Omega_{DE0} = 0.69$. In all cases the density parameters exhibit similar behaviors with those presented in the upper graph of Fig. 4.

in Fig. 11 we plot $w_{DE}(z)$ for various values of the fraction of BHs that merge. As we observe, $w_{DE}(z)$ decreases slightly as f_{merge} increases, however its effect is minor comparing to the previous parameters.

IV. CONCLUSIONS

In this work we have investigated the Wald-Gauss-Bonnet entropy in the framework of spacetime thermodynamics. The latter is a strong conjecture that connects gravity and thermodynamics, since by applying the black-hole physics in the Universe apparent horizon we can result to the Friedmann equations just starting from the first law of thermodynamics.

We have implemented the above approach in the case of Einstein-Gauss-Bonnet gravity and its corresponding Wald-Gauss-Bonnet entropy, which due to the Chern-Gauss-Bonnet theorem it is related to the Euler characteristic of the Universe topology. Nevertheless, it is known that in the case of the GB extension of general relativity, during BH merging the second law is violated. In order to remove the violation we introduced a topological link between the apparent horizon and the BH horizons, a connection that is known to hold according to holographic principle. Hence, through the gravity-thermodynamics approach we extracted modified Friedmann equations, where the new terms depend on the topology changes induced by the black-hole formation and merger. Specifically, we obtained an effective, dark energy sector of topological origin, which evolves in time according to the black-hole formation and merger rates.

In order to investigate the cosmological evolution, we estimated the BH formation rate starting from the star formation rate, and moreover we estimated the black-hole merger rate from the black-hole formation rate. Ulti-

mately, we resulted to a dark-energy energy density that depends only on the cosmic star formation rate density per redshift $\psi(z)$, which is parametrized very efficiently by the Madau-Dickinson form (38), with the remaining model parameters being the fraction of stars forming BHs f_{BH} , the fraction of black holes that eventually merge f_{merge} , the fraction of massive stars that are in binaries f_{bin} , and the average mass of progenitor stars that will evolve to form BHs $\langle m_{\text{prog}} \rangle$, as well as the GB coupling constant $\tilde{\alpha}$. The GB coupling is the only completely free parameter, since the other parameters have specific ranges according to the literature.

We investigated in detail the evolution of the dark energy and matter density parameters, of the effective dark-energy equation-of-state parameter, and of the deceleration parameter. As we saw, the Universe evolves according to the usual thermal history, with successive dark energy and matter epochs, and the transition from deceleration to acceleration takes place at $z \approx 0.6$ in agreement with observations, while at asymptotically late times the Universe results in a de Sitter phase completely dominated by dark energy. Concerning the dark-energy equation-of-state parameter, we showed that it exhibits a different behavior according to the sign and value of the GB coupling $\tilde{\alpha}$. For positive values of the GB coupling the dark energy exhibits phantom-like behavior while for negative values it exhibits quintessence-like behavior. Interestingly enough, at early and late times w_{DE} tends to the cosmological constant value -1 and the deviation happens only at intermediate redshifts, with a peak at around $z \approx 2$, a behavior that was expected since at early times there are no stars, while at asymptotically late times most black holes will have merge. Furthermore, for small absolute $\tilde{\alpha}$ values the scenario tends

to Λ CDM paradigm. Finally, we investigated the effect of the other model parameters, showing that increasing f_{BH} enhances the deviations from Λ CDM scenario, while f_{merge} has only a minor effect. Nevertheless, for the whole allowed estimated ranges of the parameters, w_{DE} remains within its observational bounds found by Planck Collaboration.

In summary, by applying the gravity-thermodynamics conjecture with the Wald entropy in the case of Einstein-Gauss-Bonnet theory, we obtained an effective, topological dark energy sector with interesting cosmological applications. Definitely, there are many investigations that need to be done before we consider the scenario at hand as a viable candidate for the description of nature. One could estimate with higher accuracy the BH merging rate per redshift, using also the future accumulating data of LIGO and VIRGO observations [85–89]. Additionally, one should use observational data from Supernova type Ia (SNIa), Baryon Acoustic Oscillations (BAO), overdensity perturbations $f\sigma_8$ and Hubble rate measurements from cosmic chronometers (CC), in order to constrain the involved parameter space. These studies lie beyond the scope of this manuscript and will be performed in future projects.

Acknowledgments

The authors would like to acknowledge the contribution of the LISA CosWG, and of COST Actions CA21136 “Addressing observational tensions in cosmology with systematics and fundamental physics (CosmoVerse)” and CA23130 “Bridging high and low energies in search of quantum gravity (BridgeQG)”.

-
- [1] A. G. Riess *et al.* (Supernova Search Team), Observational evidence from supernovae for an accelerating universe and a cosmological constant, *Astron. J.* **116**, 1009 (1998), [arXiv:astro-ph/9805201 \[astro-ph\]](#).
 - [2] S. Perlmutter *et al.* (Supernova Cosmology Project), Measurements of Omega and Lambda from 42 high redshift supernovae, *Astrophys. J.* **517**, 565 (1999), [arXiv:astro-ph/9812133 \[astro-ph\]](#).
 - [3] D. N. Spergel *et al.* (WMAP), First year Wilkinson Microwave Anisotropy Probe (WMAP) observations: Determination of cosmological parameters, *Astrophys. J. Suppl.* **148**, 175 (2003), [arXiv:astro-ph/0302209 \[astro-ph\]](#).
 - [4] M. Tegmark *et al.* (SDSS), Cosmological parameters from SDSS and WMAP, *Phys. Rev. D* **69**, 103501 (2004), [arXiv:astro-ph/0310723 \[astro-ph\]](#).
 - [5] S. W. Allen, R. W. Schmidt, H. Ebeling, A. C. Fabian, and L. van Speybroeck, Constraints on dark energy from Chandra observations of the largest relaxed galaxy clusters, *Mon. Not. Roy. Astron. Soc.* **353**, 457 (2004), [arXiv:astro-ph/0405340 \[astro-ph\]](#).
 - [6] P. Astier *et al.* (SNLS), The Supernova Legacy Survey: Measurement of Omega(M), Omega(L) and w from the first year data set, *Astron. Astrophys.* **447**, 31 (2006), [arXiv:astro-ph/0510447 \[astro-ph\]](#).
 - [7] E. J. Copeland, M. Sami, and S. Tsujikawa, Dynamics of dark energy, *Int. J. Mod. Phys. D* **15**, 1753 (2006), [arXiv:hep-th/0603057 \[hep-th\]](#).
 - [8] Y.-F. Cai, E. N. Saridakis, M. R. Setare, and J.-Q. Xia, Quintom Cosmology: Theoretical implications and observations, *Phys. Rept.* **493**, 1 (2010), [arXiv:0909.2776 \[hep-th\]](#).
 - [9] E. N. Saridakis *et al.* (CANTATA), *Modified Gravity and Cosmology. An Update by the CANTATA Network*, edited by E. N. Saridakis, R. Lazkoz, V. Salzano, P. Vargas Moniz, S. Capozziello, J. Beltrán Jiménez, M. De Laurentis, and G. J. Olmo (Springer, 2021) [arXiv:2105.12582 \[gr-qc\]](#).
 - [10] S. Capozziello and M. De Laurentis, Extended Theories of Gravity, *Phys. Rept.* **509**, 167 (2011), [arXiv:1108.6266 \[gr-qc\]](#).
 - [11] Y.-F. Cai, S. Capozziello, M. De Laurentis, and E. N. Saridakis, f(T) teleparallel gravity and cosmology, *Rept.*

- Prog. Phys. **79**, 106901 (2016), arXiv:1511.07586 [gr-qc].
- [12] S. Nojiri, S. D. Odintsov, and V. K. Oikonomou, Modified Gravity Theories on a Nutshell: Inflation, Bounce and Late-time Evolution, *Phys. Rept.* **692**, 1 (2017), arXiv:1705.11098 [gr-qc].
- [13] R. Alves Batista *et al.*, White Paper and Roadmap for Quantum Gravity Phenomenology in the Multi-Messenger Era, (2023), arXiv:2312.00409 [gr-qc].
- [14] A. Addazi *et al.*, Quantum gravity phenomenology at the dawn of the multi-messenger era—A review, *Prog. Part. Nucl. Phys.* **125**, 103948 (2022), arXiv:2111.05659 [hep-ph].
- [15] K. S. Stelle, Renormalization of Higher Derivative Quantum Gravity, *Phys. Rev. D* **16**, 953 (1977).
- [16] B. Zwiebach, Curvature Squared Terms and String Theories, *Phys. Lett. B* **156**, 315 (1985).
- [17] D. G. Boulware and S. Deser, String Generated Gravity Models, *Phys. Rev. Lett.* **55**, 2656 (1985).
- [18] D. J. Gross and J. H. Sloan, The Quartic Effective Action for the Heterotic String, *Nucl. Phys. B* **291**, 41 (1987).
- [19] C. Vafa and E. Witten, A Strong coupling test of S duality, *Nucl. Phys. B* **431**, 3 (1994), arXiv:hep-th/9408074 [hep-th].
- [20] T. Jacobson, Thermodynamics of Spacetime: The Einstein Equation of State, *Phys. Rev. Lett.* **75**, 1260 (1995), arXiv:gr-qc/9504004 [gr-qc].
- [21] T. Padmanabhan, Gravity and the Thermodynamics of Horizons, *Phys. Rept.* **406**, 49 (2005), arXiv:gr-qc/0311036 [gr-qc].
- [22] T. Padmanabhan, Thermodynamical Aspects of Gravity: New insights, *Rept. Prog. Phys.* **73**, 046901 (2010), arXiv:0911.5004 [gr-qc].
- [23] G. W. Gibbons and S. W. Hawking, Cosmological Event Horizons, Thermodynamics, and Particle Creation, *Phys. Rev. D* **15**, 2738 (1977).
- [24] R.-G. Cai and S. P. Kim, First law of thermodynamics and Friedmann equations of Friedmann-Robertson-Walker universe, *JHEP* **02**, 050, arXiv:hep-th/0501055 [hep-th].
- [25] M. Akbar and R.-G. Cai, Thermodynamic behavior of the Friedmann equation at the apparent horizon of the FRW universe, *Phys. Rev. D* **75**, 084003 (2007), arXiv:hep-th/0609128 [hep-th].
- [26] R.-G. Cai and L.-M. Cao, Unified first law and thermodynamics of apparent horizon in FRW universe, *Phys. Rev. D* **75**, 064008 (2007), arXiv:gr-qc/0611071 [gr-qc].
- [27] A. Paranjape, S. Sarkar, and T. Padmanabhan, Thermodynamic route to field equations in Lanczos-Lovelock gravity, *Phys. Rev. D* **74**, 104015 (2006), arXiv:hep-th/0607240 [hep-th].
- [28] A. Sheykhi, B. Wang, and R.-G. Cai, Thermodynamical properties of apparent horizon in warped DGP braneworld, *Nucl. Phys. B* **779**, 1 (2007), arXiv:hep-th/0701198 [hep-th].
- [29] M. Akbar and R.-G. Cai, Thermodynamic behavior of field equations for f(R) gravity, *Phys. Lett. B* **635**, 7 (2006), arXiv:hep-th/0602156 [hep-th].
- [30] M. Jamil, E. N. Saridakis, and M. R. Setare, Thermodynamics of dark energy interacting with dark matter and radiation, *Phys. Rev. D* **81**, 023007 (2010), arXiv:0910.0822 [hep-th].
- [31] R.-G. Cai and N. Ohta, Horizon thermodynamics and gravitational field equations in Horava-Lifshitz gravity, *Phys. Rev. D* **81**, 084061 (2010), arXiv:0910.2307 [hep-th].
- [32] M. Wang, J. Jing, C. Ding, and S. Chen, First law of thermodynamics in IR modified Horava-Lifshitz gravity, *Phys. Rev. D* **81**, 083006 (2010), arXiv:0912.4832 [gr-qc].
- [33] M. Jamil, E. N. Saridakis, and M. R. Setare, Holographic dark energy with varying gravitational constant, *JCAP* **11**, 032, arXiv:1003.0876 [hep-th].
- [34] Y. Gim, W. Kim, and S.-H. Yi, The first law of thermodynamics in Lifshitz black holes revisited, *JHEP* **07**, 002, arXiv:1403.4704 [hep-th].
- [35] Z.-Y. Fan and H. Lu, Thermodynamical first laws of black holes in quadratically-extended gravities, *Phys. Rev. D* **91**, 064009 (2015), arXiv:1501.00006 [hep-th].
- [36] A. Lymperis and E. N. Saridakis, Modified cosmology through nonextensive horizon thermodynamics, *Eur. Phys. J. C* **78**, 993 (2018), arXiv:1806.04614 [gr-qc].
- [37] E. N. Saridakis, Barrow holographic dark energy, *Phys. Rev. D* **102**, 123525 (2020), arXiv:2005.04115 [gr-qc].
- [38] S. Basilakos, A. Lymperis, M. Petronikolou, and E. N. Saridakis, Alleviating both H_0 and σ_8 tensions in Tsallis cosmology, *Eur. Phys. J. C* **84**, 297 (2024), arXiv:2308.01200 [gr-qc].
- [39] R. M. Wald, Black hole entropy is the Noether charge, *Phys. Rev. D* **48**, R3427 (1993), arXiv:gr-qc/9307038.
- [40] V. Iyer and R. M. Wald, Some properties of Noether charge and a proposal for dynamical black hole entropy, *Phys. Rev. D* **50**, 846 (1994), arXiv:gr-qc/9403028.
- [41] C. Lanczos, A Remarkable property of the Riemann-Christoffel tensor in four dimensions, *Annals Math.* **39**, 842 (1938).
- [42] D. Lovelock, The Einstein tensor and its generalizations, *J. Math. Phys.* **12**, 498 (1971).
- [43] T. Jacobson and R. C. Myers, Black hole entropy and higher curvature interactions, *Phys. Rev. Lett.* **70**, 3684 (1993), arXiv:hep-th/9305016.
- [44] S. Shen Chern, On the curvatura integra in a riemannian manifold, *Annals of Mathematics* **46**, 674 (1945).
- [45] M. Nakahara, *Geometry, topology and physics* (2003).
- [46] S. A. Tsilioukas, E. N. Saridakis, and C. Tzerefos, Dark energy from topology change induced by microscopic Gauss-Bonnet wormholes, *Phys. Rev. D* **109**, 084010 (2024), arXiv:2312.07486 [gr-qc].
- [47] S. Tsilioukas and E. Saridakis, Dark Energy from topology change at the foam level, *PoS CORFU2023*, 182 (2024).
- [48] S. Sarkar and A. C. Wall, Second Law Violations in Lovelock Gravity for Black Hole Mergers, *Phys. Rev. D* **83**, 124048 (2011), arXiv:1011.4988 [gr-qc].
- [49] B. Farb and D. Margalit, *A Primer on Mapping Class Groups*, Princeton Mathematical Series, Vol. 49 (Princeton University Press, 2012).
- [50] G. 't Hooft, Dimensional Reduction in Quantum Gravity, *Conf. Proc. C* **930308**, 284 (1993), arXiv:gr-qc/9310026 [gr-qc].
- [51] L. Susskind, The World as a hologram, *J. Math. Phys.* **36**, 6377 (1995), arXiv:hep-th/9409089.
- [52] W. Fischler and L. Susskind, Holography and cosmology, (1998), arXiv:hep-th/9806039.
- [53] R. Bousso, The Holographic principle, *Rev. Mod. Phys.* **74**, 825 (2002), arXiv:hep-th/0203101.
- [54] P. Horava and D. Minic, Probable values of the cosmological constant in a holographic theory, *Phys. Rev. Lett.* **85**, 1610 (2000), arXiv:hep-th/0001145.

- [55] M. Li, A Model of holographic dark energy, *Phys. Lett. B* **603**, 1 (2004), [arXiv:hep-th/0403127](#).
- [56] S. Wang, Y. Wang, and M. Li, Holographic Dark Energy, *Phys. Rept.* **696**, 1 (2017), [arXiv:1612.00345 \[astro-ph.CO\]](#).
- [57] Q.-G. Huang and M. Li, The Holographic dark energy in a non-flat universe, *JCAP* **08**, 013, [arXiv:astro-ph/0404229](#).
- [58] D. Pavon and W. Zimdahl, Holographic dark energy and cosmic coincidence, *Phys. Lett. B* **628**, 206 (2005), [arXiv:gr-qc/0505020](#).
- [59] B. Wang, Y.-g. Gong, and E. Abdalla, Transition of the dark energy equation of state in an interacting holographic dark energy model, *Phys. Lett. B* **624**, 141 (2005), [arXiv:hep-th/0506069](#).
- [60] S. Nojiri and S. D. Odintsov, Unifying phantom inflation with late-time acceleration: Scalar phantom-nonphantom transition model and generalized holographic dark energy, *Gen. Rel. Grav.* **38**, 1285 (2006), [arXiv:hep-th/0506212](#).
- [61] M. Li, X.-D. Li, S. Wang, and X. Zhang, Holographic dark energy models: A comparison from the latest observational data, *JCAP* **06**, 036, [arXiv:0904.0928 \[astro-ph.CO\]](#).
- [62] M. R. Setare and E. N. Saridakis, Non-minimally coupled canonical, phantom and quintom models of holographic dark energy, *Phys. Lett. B* **671**, 331 (2009), [arXiv:0810.0645 \[hep-th\]](#).
- [63] M. R. Setare and E. N. Saridakis, Correspondence between Holographic and Gauss-Bonnet dark energy models, *Phys. Lett. B* **670**, 1 (2008), [arXiv:0810.3296 \[hep-th\]](#).
- [64] E. N. Saridakis, Ricci-Gauss-Bonnet holographic dark energy, *Phys. Rev. D* **97**, 064035 (2018), [arXiv:1707.09331 \[gr-qc\]](#).
- [65] E. N. Saridakis, K. Bamba, R. Myrzakulov, and F. K. Anagnostopoulos, Holographic dark energy through Tsallis entropy, *JCAP* **12**, 012, [arXiv:1806.01301 \[gr-qc\]](#).
- [66] N. Drepanou, A. Lymperis, E. N. Saridakis, and K. Yesmakhanova, Kaniadakis holographic dark energy and cosmology, *Eur. Phys. J. C* **82**, 449 (2022), [arXiv:2109.09181 \[gr-qc\]](#).
- [67] S. W. Hawking, Gravitational radiation from colliding black holes, *Phys. Rev. Lett.* **26**, 1344 (1971).
- [68] F. Iacovelli, M. Mancarella, S. Foffa, and M. Maggiore, Forecasting the Detection Capabilities of Third-generation Gravitational-wave Detectors Using GWFAST, *Astrophys. J.* **941**, 208 (2022), [arXiv:2207.02771 \[gr-qc\]](#).
- [69] I. Gupta *et al.*, Characterizing Gravitational Wave Detector Networks: From A[#] to Cosmic Explorer, (2023), [arXiv:2307.10421 \[gr-qc\]](#).
- [70] L. Lehoucq, I. Dvorkin, R. Srinivasan, C. Pellouin, and A. Lamberts, Astrophysical uncertainties in the gravitational-wave background from stellar-mass compact binary mergers, *Mon. Not. Roy. Astron. Soc.* **526**, 4378 (2023), [arXiv:2306.09861 \[astro-ph.HE\]](#).
- [71] P. Madau and M. Dickinson, Cosmic Star Formation History, *Ann. Rev. Astron. Astrophys.* **52**, 415 (2014), [arXiv:1403.0007 \[astro-ph.CO\]](#).
- [72] E. E. Salpeter, The Luminosity Function and Stellar Evolution, *Astrophys. J.* **121**, 161 (1955).
- [73] A. Heger and S. E. Woosley, The Nucleosynthetic signature of population III, *Astrophys. J.* **567**, 532 (2002), [arXiv:astro-ph/0107037 \[astro-ph\]](#).
- [74] C. L. Fryer, K. Belczynski, G. Wiktorowicz, M. Dominik, V. Kalogera, and D. E. Holz, Compact Remnant Mass Function: Dependence on the Explosion Mechanism and Metallicity, *Astrophys. J.* **749**, 91 (2012), [arXiv:1110.1726 \[astro-ph.SR\]](#).
- [75] S. E. Woosley, A. Heger, and T. A. Weaver, The evolution and explosion of massive stars, *Rev. Mod. Phys.* **74**, 1015 (2002).
- [76] T. Sukhbold, T. Ertl, S. E. Woosley, J. M. Brown, and H.-T. Janka, Core-collapse Supernovae from 9 to 120 Solar Masses Based on Neutrino-powered Explosions, *Astrophys. J.* **821**, 38 (2016), [arXiv:1510.04643 \[astro-ph.SR\]](#).
- [77] A. Boesky, F. S. Broekgaarden, and E. Berger, The Binary Black Hole Merger Rate Deviates From the Cosmic Star Formation Rate: A Tug of War Between Metallicity and Delay Times, (2024), [arXiv:2405.01623 \[astro-ph.HE\]](#).
- [78] H. Sana *et al.*, Binary Interaction Dominates the Evolution of Massive Stars, *Science* **337**, 444 (2012).
- [79] K. Belczynski, D. E. Holz, T. Bulik, and R. O'Shaughnessy, The First Gravitational-Wave Source from the Isolated Evolution of Two 40-100 M_⊙ Stars, *Nature* **534**, 512 (2016), [arXiv:1602.04531 \[astro-ph.HE\]](#).
- [80] J. J. Eldridge and E. R. Stanway, BPASS predictions for binary black hole mergers, *Mon. Not. Roy. Astron. Soc.* **462**, 3302 (2016), [arXiv:1602.03790 \[astro-ph.HE\]](#).
- [81] M. Dominik *et al.*, Double Compact Objects. I. The Significance of the Common Envelope on Merger Rates, *Astrophys. J.* **759**, 52 (2012), [arXiv:1202.4901 \[astro-ph.SR\]](#).
- [82] M. Moe and R. Di Stefano, Mind Your Ps and Qs: The Interrelation between Periods, Mass Ratios, and Orbital Planes for Binary Stars, *Astrophys. J. Suppl.* **230**, 15 (2017), [arXiv:1606.05347 \[astro-ph.SR\]](#).
- [83] G. Duchene and A. Kraus, Stellar Multiplicity, *Ann. Rev. Astron. Astrophys.* **51**, 269 (2013), [arXiv:1303.3028 \[astro-ph.SR\]](#).
- [84] N. Aghanim and others [Planck Collaboration], Planck 2018 results. VI. Cosmological parameters, *Astron. Astrophys.* **641**, A6 (2020), [arXiv:1807.06209 \[astro-ph.CO\]](#).
- [85] G. Fragione, N. W. C. Leigh, I. Ginsburg, and B. Kocsis, Formation of LISA Black Hole Binaries in Merging Dwarf Galaxies: the Impact of Star Formation and Dynamics, *Astrophys. J. Lett.* **864**, L19 (2018), [arXiv:1806.11112 \[astro-ph.GA\]](#).
- [86] J. Ellis, M. Lewicki, V. Vaskonen, and N. Zheng, Probing Supermassive Black Hole Seed Scenarios with Gravitational-wave Measurements, *JCAP* **06**, 024, [arXiv:2004.08428 \[astro-ph.CO\]](#).
- [87] E. Barausse, I. Dvorkin, M. Tremmel, M. Volonteri, and M. Bonetti, Massive black hole merger rates: the effect of kpc separation wandering and supernova feedback, *Mon. Not. Roy. Astron. Soc.* **503**, 5333 (2021), [arXiv:2006.03065 \[astro-ph.GA\]](#).
- [88] S. Banks, K. Lee, N. Azimi, K. Scarborough, N. Stefanov, I. Periwal, C. DeGraf, and T. Di Matteo, On the detectability of massive black hole merger events by LISA, *Mon. Not. Roy. Astron. Soc.* **507**, 114 (2021), [arXiv:2107.09084 \[astro-ph.GA\]](#).
- [89] K. Li, T. Bogdanović, D. R. Ballantyne, and M. Bonetti, Massive Black Hole Binaries from the TNG50-3 Simu-

lation: I. Coalescence and LISA Detection Rates, *Mon.*

Not. Roy. Astron. Soc. **511**, 608 (2022), [arXiv:2201.11088](https://arxiv.org/abs/2201.11088) [astro-ph.GA].